



## MICROSTRUCTURAL CHARACTERIZATION OF SECONDARY PHASES OF TI-AL BASED ALLOYS BY TRANSMISSION ELECTRON MICROSCOPY

María Victoria Castro Riglos (1), Jonathan Paul (2), Florian Pyczak (2).

(1) División Física de Metales, Centro Atómico Bariloche, S.C de Bariloche, Argentina & CONICET. (2) Helmholtz Zentrum Geesthacht (HZG), Metal Physics Department, Geesthacht, Germany.  
Email: victoria.castroriglos@cab.cnea.gov.ar

Automotive and aerospace industries are always looking for innovative light weight materials that offer good performance even under high temperature conditions. Within this group, one of the most promising materials are intermetallic Ti-Al based alloys. Besides their low density, the advantages presented by this class of alloys are their good strength and creep properties up to 750 °C, their high oxidation resistance and good thermal conductivities [1]. However, there exist some inconveniences associated with this kind of alloys like low ductility and toughness at room temperature, poor workability, and limited high temperature strength [2].

One approach to increase the high temperature strength is to introduce other elements that can precipitate into small particles during annealing, so modifying the microstructure (morphology, volume fraction, distribution and density of the particles within the alloy matrix), the stability between phases and the specific mechanical properties [3]. Two additions that are already recognized as enhancers for the mechanical behavior are: (i) Niobium, due to its favorable effect on creep and oxidation resistance; and (ii) Carbon because it can strengthen by precipitation of secondary phases or by solid solution strengthening [3]. Silicon may be included within this second type of additions but there are still limited studies on the effects of Silicon in Ti-Al alloys. For this reason, in the present work it was analyzed how the mechanical properties and microstructure are affected by Si addition.

With this aim two alloy systems were studied: Ti-45Al-5Nb-1Si-0.5C (Type I) and Ti-45Al-5Nb-1Si (Type II), at.%. Each alloy was studied in its “As-cast” state (AC) and after heat treatment (HT) at 800°C over a week.

Vickers Micro Hardness measurements were performed using a Mitutoyo Hardness Testing machine with a load of 1kgf. The microstructure was characterized in a FEI Tecnai G2 transmission electron microscope. Also, some computer simulations were carried out by JEMS 4 software in order to verify which phases were present in each case.

Comparing to previous studies [3], results obtained from hardness measurements (Table 1) showed for both systems a remarkable increase in hardness with respect to other equivalent Si free systems (hardness increased by around 100-150 HV units). On the other hand, when comparing Type I and Type II alloys there was a slight increment when both additions (C and Si) were present.

By TEM observations it was established that all alloys exhibited a lamellar microstructure typical for the Ti-45Al-5Nb base composition. The lamellar microstructure consists of alternating  $\alpha_2$  and  $\gamma$  lamellas. One example is shown in Fig. 1, where a typical image of the Type I (HT) alloy is presented. Unlike a typical Ti-45Al-5Nb alloy microstructure, many precipitates from a new phase can be seen that are usually located at  $\alpha_2/\gamma$  interfaces (pointed with orange arrows). In order to determine the type of these precipitates High Resolution TEM images were recorded, as the one displayed in Fig. 2A. Fig. 2B shows a detail of the enclosed area in Fig. 2A. From right to left, three different crystalline regions can be observed. By performing a Fast Fourier Transform (FFT) in each region an image equivalent to a diffraction pattern (DP) is obtained. These FFTs were compared to simulated diffraction patterns for  $\alpha_2$  and  $\gamma$  phases. From this comparison it was determined that the structure on the left-side in Fig. 2A was  $\alpha_2$  in [100] zone axis condition (Fig. 3A and 3D), and the right-side region corresponds to  $\gamma$  phase in [101] ZA condition (Fig. 3C and F).

The FFT from the unknown structure was compared to simulated patterns for silicides ( $\text{Ti}_5\text{Si}_3$ ) which was the most likely phase to appear here. The results showed a very good agreement between FFT and the simulated DP for  $\text{Ti}_5\text{Si}_3$  in [2 -7 -8] zone axis (Fig. 3B and E).

## REFERENCES

- [1] Clemens H., Mayer S., (2013), "Design, Processing, Microstructure, Properties, and Applications of Advanced Intermetallic TiAl Alloys", *Advanced Engineering Materials*, 15 (4) 191:215.
- [2] Appel F., Paul J.D.H., Oehring M., (2011), "*Gamma Titanium Aluminide Alloys: Science and Technology*", Wiley-VCH; 1<sup>st</sup> edition.
- [3] Gabrisch H., Stark A., Schimansky F.P., Wang L., Schell N., Lorenz U., Pyczak F., (2013), "Investigation of carbides in Ti-45Al-5Nb-xC alloys ( $0 \leq x \leq 1$ ) by transmission electron microscopy and high energy-XRD", *Intermetallics*, 33, 44:53.

## ACKNOWLEDGMENTS

The authors thank to the DAAD for the fellowship that provided financial support. Also Metal Physics Division from HZG and CAB are acknowledged for the use of TEM facilities.

**Table 1:** Vickers Micro Hardness for each system and its heat treatment.

Alloy System	HV $\pm$ $\Delta$ HV	
	AC	HT
Type I	490 $\pm$ 10	500 $\pm$ 10
Type II (no C content)	475 $\pm$ 9	472 $\pm$ 8

## FIGURES

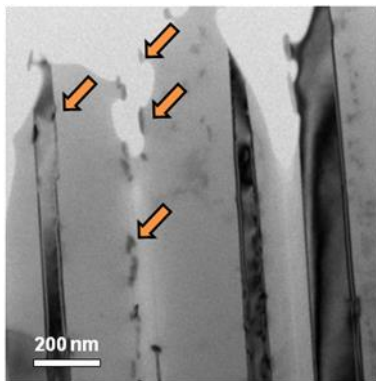


**Figure 1:** Type I (HT) specimen microstructure. Lamellar  $\alpha/\gamma$  and interfacial precipitates are observed.

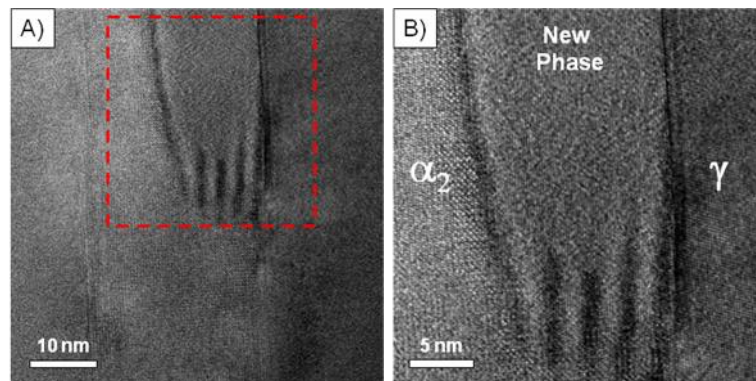


**Figure 2:** HRTEM images. A) Overview of a precipitate formed within a lamellar interface. B) Detail of the area within the square in 2A.

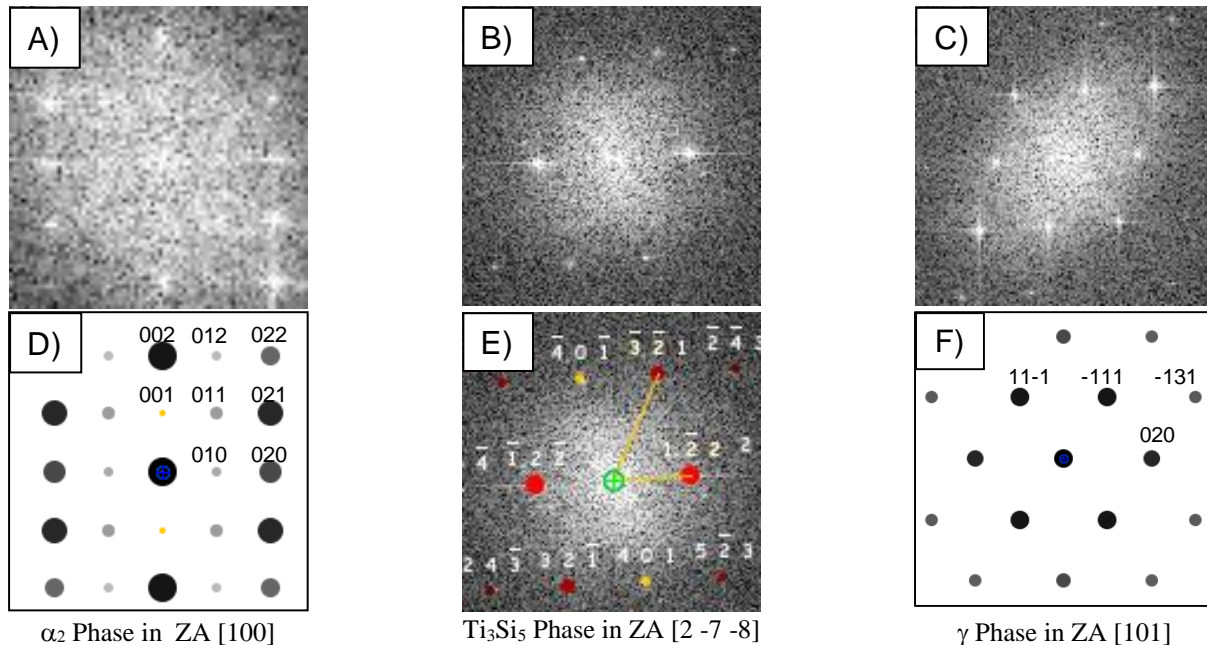


**Figure 3:** Images A, B and C present the FFT from each region in Figure 2B. D and F display simulated DP's that correspond to Figure 3A and 3C, respectively. Fig. 3E shows the simulated DP for  $Ti_3Si_5$  structure superimposed to FFT (3B) that presented the best match. All the images are  $18.5 \text{ nm}^{-1}$  wide.